Low-Energy Electron Microscopy: Imaging Surface Dynamics

Flexibility and time resolution make LEEM a powerful tool for studying mesoscale phenomena—from surface diffusion to magnetization.

Raymond J. Phaneuf and Andreas K. Schmid

n 1985, Ernst Bauer and his student Wolfgang Telieps published a stunning set of images that abruptly solved a long-debated question in surface science: What is the nature of the phase transition that occurs on the (111) surface of silicon?1 Determining the complex ordered arrangement of atoms, or "reconstruction," that occurs there had been one of the hottest problems in surface science for nearly 25 years.2 One of their images (see figure 1) shows a sharply defined coexistence between two structural phases and demonstrates a first-order—rather than a continuous second-order-transition between an ordered (bright) and disordered (dark) arrangement of atoms at the surface. Bauer and Telieps's unambiguous answer about the nature of that disordering transition dramatically introduced a very powerful probe of solid surfaces: low-energy electron microscopy (LEEM).

Since publication of those early images, an increasing number of investigators have used LEEM to gain insights into a variety of dynamical processes on surfaces. After all, whether the interest is crystal growth, catalysis, or thinfilm or multilayer materials engineering, surface science is based on understanding surfaces not as static objects, but as dynamic systems. Key questions include, How do structural transitions nucleate and propagate across a surface? What are the limiting processes in atom transport across a surface during temperature treatments or material deposition?

At roughly the same time that successful LEEM research began, scanning tunneling microscopy burst on the scene as an important technique in surface science. Although STM, with its subnanometer resolution, was well suited for examining surface structures and atomic arrangements, LEEM, with its large field of view and fast imaging rate, was well poised for studying dynamics.

LEEM combines a number of spectroscopic techniques and uses the fact—already exploited in low-energy electron diffraction—that electrons with energies of a few to a few tens of eV are extremely sensitive to near-surface atomic order. Depending on the energy of the incident electron beam, subtle differences in local atomic structure or

Raymond Phaneuf is an assistant professor in the Department of Materials and Nuclear Engineering and the Laboratory for the Physical Sciences at the University of Maryland, College Park. Andreas Schmid is a staff scientist at the National Center for Electron Microscopy, Lawrence Berkeley National Laboratory, in Berkeley, California.

composition can give rise to dramatic contrast in LEEM images. An example is the contrast, evident in figure 1, that results from a strong difference in the specularly diffracted intensity between ordered and disordered structures. What distinguishes LEEM from LEED and scattering techniques is its real-time surface imaging capability

(although the diffraction pattern is still available in the back focal plane of the objective lens). Image formation with electrons is analogous to light-microscope imaging. The backscattered electron beam diverges and refocuses through electrostatic and magnetic lenses on its way to a phosphor screen (see the box on page 52). LEEM is the fruit of more than 20 years of work by Bauer, who recognized by the early 1960s that the high reflectivity of lowenergy electrons from surfaces would make surface-sensitive imaging practical. The first published images caused great excitement in the surface science community because they were acquired with high spatial resolution, typically several nanometers, and at video rates. LEEM can image in situ samples over a wide range of temperatures and in the presence of incident fluxes of atoms, ions, or light. That flexibility allows researchers to more easily control the evolution of nanostructures.

Cobalt on silicon

Bauer and Telieps's initial observation of phase coexistence became the starting point for a growing number of discoveries using LEEM. One crucial problem in modifying surfaces is determining how the deposition of different types of atoms influences the structures that form and coexist. For example, one of us (Phaneuf) and Peter Bennett at Arizona State University used LEEM to investigate the structures that evolve when a very small flux of cobalt adsorbs onto the Si(111) surface at elevated temperatures.3 Our results demonstrated an interesting consequence of certain impurities on the transition: a stabilization of the disordered phase below the clean-surface transition temperature. Starting with a single-phase (7×7) ordered surface (figure 2a), Co segregated to steps and domain boundaries of the ordered structure (figure 2b). Further deposition—up to a tenth of a monolayer—caused the disordered Co-containing structure to spread outward, leaving an almost entirely dark image. Previous STM measurements suggest that the disordered, so-called " (1×1) ," regions contain a random arrangement of Co-containing clusters and individual Si adatoms decorating a bulklike surface termination.4 The disordered structure visibly grew outward from steps and domain boundaries at the expense of the ordered regions when either the Co coverage was increased at a fixed temperature or when the temperature was raised at a fixed Co coverage. Images recorded while heating or cooling the surface revealed that the transition was reversible, so that a local equilibrium

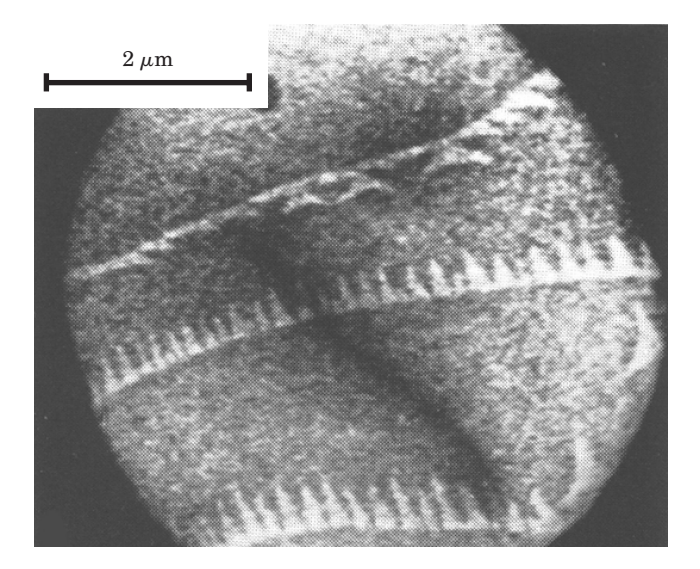


Figure 1. Coexisting phases on the (111) surface of silicon observed with low-energy electron microscopy. The contrast between light and dark regions illustrates the sharp division between the phases. Bright regions are ordered, with a unit cell seven times as large as the bulk Si spacing in each of the two high-symmetry directions—referred to as (7×7) reconstructed—and darker regions contain a disordered lattice gas of Si atoms. That surface-disordered structure is referred to as a " (1×1) " phase, because of periodicity below the top layer. The dark diagonal line is a crack in the detector. (Adapted from ref. 1.)

existed between phases.

That insight about the transition would have been almost impossible to deduce from diffraction studies alone because the disordered structure produces no extra reflections in the diffraction pattern. Increasing the Co coverage produces a large and continuous change of the transition temperature, with a depression of 170°C resulting from only a tenth of a monolayer. The driving force is well known from bulk alloy systems: Adding an insoluble impurity to a solid phase lowers its melting point and allows the impurity to segregate to the liquid phase, in which its solubility is higher. In our case, lowering the disordering temperature allowed Co-containing clusters to segregate out of the ordered surface regions into the disordered phase. The shape of the phase boundary in figure 2c indicates the presence of a small repulsion between the Cocontaining particles in the disordered phase.

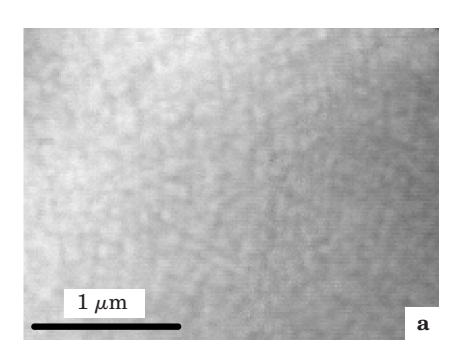
Even for atomically clean Si(111) surfaces, the fact that there are coexisting ordered and disordered regions at all is surprising. At first, such coexistence seems at odds with the Gibbs phase rule, which predicts that only a single phase should exist at a given temperature and pressure, with sharp transitions between phases. Using

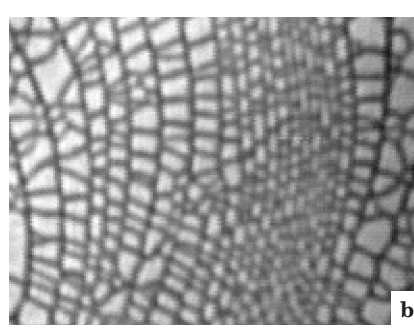
LEEM, Jim Hannon and his collaborators at IBM⁵ recently discovered that long-range interactions between phase boundaries preclude a sharp transition between phases, even when the defect-free regions of the surface are arbitrarily large—the so-called thermodynamic limit. The nature of the domain boundary interactions can stem either from the two phases having different surface stresses or from their having different work functions. The temperature dependence of the relative sizes of the two types of regions on the surface are consistent with a model that includes a term in the free energy corresponding to the elastic interaction between "force monopoles" at the boundaries between phases.

Step dynamics

The use of LEEM has progressed gradually, from qualitative imaging to fully quantitative analysis. The almost unique ability of the LEEM to form real-time images over a wide range of temperatures and conditions allows researchers to extract thermodynamic quantities that would be difficult, if not impossible, to obtain using other techniques.

Consider the work of Ruud Tromp and his collaborators at IBM.6 Those researchers observed the Brownian





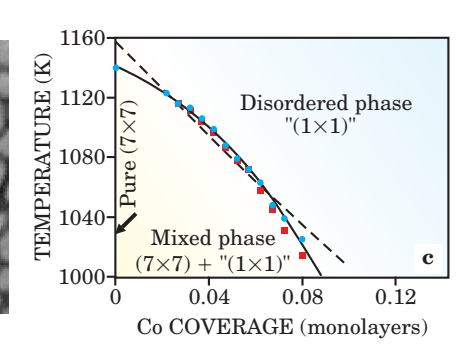


Figure 2. Cobalt on silicon(111). (a) From its diffraction pattern the clean Si surface was confirmed to be an ordered (7×7) reconstruction. (b) After 0.02 monolayer of cobalt had been adsorbed, the dark regions appeared. They were a disordered lattice-gas arrangement of cobalt-containing clusters that segregated to steps (the longer lines) and domain boundaries (the shorter lines). (c) A clear phase boundary separates a region of phase coexistence from a pure disordered phase. Blue dots indicate the temperatures at which the surface entirely disorders on heating, and red squares indicate the temperatures at which the phase coexistence appears on cooling. The solid curve shows a fit to the Clapeyron equation, including a repulsive interaction between Co-containing clusters in the disordered phase. The dashed straight line represents the noninteracting case. (Adapted from ref. 3.)

The Basic Principles of LEEM

ow does an electron microscope work? Essentially, electrostatic or magnetic lenses focus an electron beam onto a sample to illuminate a certain field of view; the scattered electrons are then collected and refocused onto a phosphor screen to form an image. What distinguishes low-energy electron microscopes (LEEMs) from the crowd is the energy range of the illuminating electrons, which are reduced to between 1 and 100 eV—far less than the 100 000 eV typically used in the

common transmission electron microscopes (TEMs). The useful energy ranges for these two techniques differ by many orders of magnitude cause they exploit different scattering angles. High-energy electrons scatter through small angles, and the dominance of that forward scattering allows electrons to penetrate thin samples for

Sample $(V = -V_0 + V_s)$ Objective lens

Magnetic prism $(V = -V_0)$ Condenser lenses

Projector lenses

Detector

investigations of a sample's interior structures. In LEEM, a reflection geometry is more suitable: Low-energy electrons scatter through large angles, making backscattering intensities high. At normal incidence, for instance, it is common for crystalline samples illuminated with electrons of just a few eV to elastically reflect a substantial fraction of the electrons (sometimes nearly all of them!) straight back toward the electron source. That reflectance explains the attractiveness of low-energy electron beams for making high-brightness images of surface structures.

Nevertheless, the backscattering geometry has been a challenge for LEEM instrumentation design. The column containing the illumination optics and the column containing the imaging optics both have to be arranged in front of the sample surface. In fact, for best imaging conditions, the illuminating beam and the reflected-image beam often share a common optical axis in the direction normal to the sample surface. Therefore, a beam-separation element is needed somewhere along that optical axis. In most LEEMs, a magnetic field (**B** in the figure) bends the illuminating beam (green) onto the axis normal to the sample surface. Electrons reflected from the sample (yellow) travel back on the same axis to again reach the prism, where they deflect further into an imaging column that is separate from the illumination column (see the figure).

The practicality of building a microscope that operates at energies of a few eV has also been a challenge. Electron-optical lenses focus electrons poorly at energies much less than 10 keV due to the variation in focal length with energy and the energy spread associated with practical electron sources. The blurring that results is proportional to the ratio of the energy spread to the average energy and thus increases as the reciprocal of the energy. Ernst Bauer solved that problem by combining conventional, moderately high-energy electron optics (focusing the beam, at V_0) with a special objective lens that decelerates the incident electrons in the last few millimeters be-

fore they reach the sample, and reaccelerates the reflected electrons before they are refocused. Thus, the sample, which is reverse-biased at $V_{\rm c}$, sits in a strong electrostatic field and becomes an integral part of the imaging optics. Bauer predicted that the imaging properties of this electrostatic field should limit the resolution achievable by the objec-

tive lens and, consequently, of the entire microscope. Numerical calculations using typical values of sample–lens separations, field strengths, and energy spreads yielded a predicted optimum resolution in conventional LEEM instruments of approximately 35 Å.

The sensitivity of low-energy electrons to near-surface atomic layers explains their appeal and governs the image contrast in LEEM. High-energy electrons used, say, in TEM, penetrate deeply into the electronic shells of atoms and make the nuclear charge of the atoms one of the most important factors influencing TEM contrast. In LEEM, the lowenergy electrons never get close to atomic nuclei; rather, the detailed structure of the outer electron shells of atoms near the sample surface determines image contrast. Chemical bonds between atoms are an example of the electronic structure in outer electron shells; indeed, LEEM image contrast depends very sensitively on subtle differences in the chemical composition or crystal structure of the topmost atomic layers. An image's bright and dark areas for an ordered surface come in part from satisfying or not satisfying the Bragg condition, leading to large variations in intensity with incident energy; for disordered structures the variations and maximum intensity are considerably smaller. Defects such as atomic height steps or dislocations and phenomena such as quantum well states in thin films can often be imaged with very good contrast. Or, if a spin-polarized electron beam illuminates the surface (from so-called SPLEEM instruments), surface-magnetization directions show contrast.

motion of monolayer surface steps and studied the evolution of monolayer islands on the (001) surface of Si. Both phenomena are mediated by the attachment and detachment of Si atoms from the edges of the steps or islands and by their diffusion across the surface. Which of the activated atomic mechanisms is rate limiting, attachment/detachment or diffusion? Thermodynamics distinguishes the two cases based on a statistical analysis of the Fourier components of the spatial and temporal correlations along a fluctuating step edge. In particular, the amplitude A(q)

of the Fourier component corresponding to the wavevector $q=2\pi/\lambda$ should be inversely proportional to λ^2 if attachment/detachment is rate limiting, but to λ^3 if, instead, fluctuations result from a diffusion-limited process. (See discussions in the articles by Zoltán Toroczkai and Ellen D. Williams, Physics Today, December 1999, page 24, and by Harold Zandvliet, Bene Poelsema and Brian Swartzentruber, Physics Today, July 2001, page 40.)

In an impressively detailed analysis, Norm Bartelt used more than 35×10^6 step-edge positions from image se-

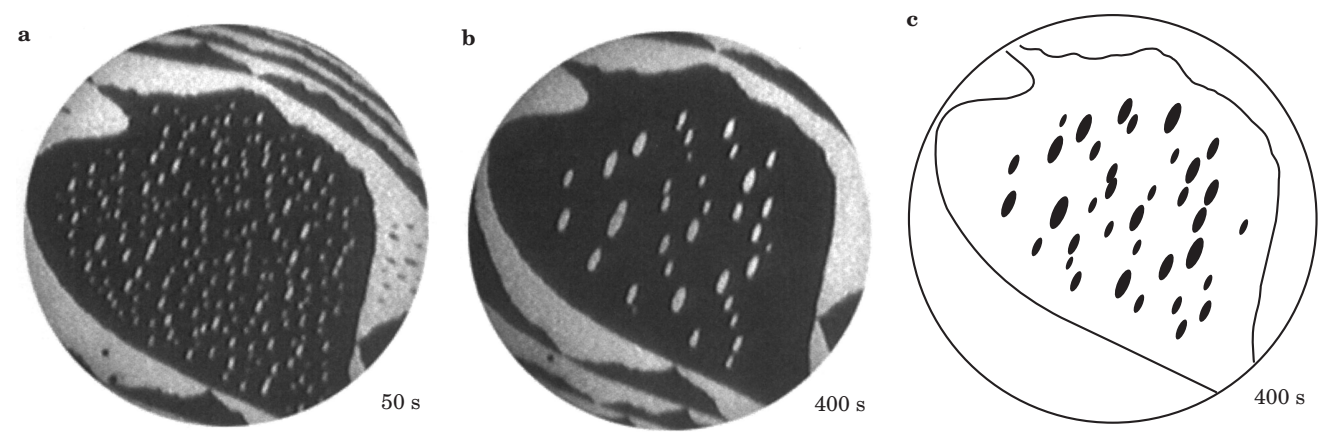


Figure 3. Atomistic diffusion on silicon. Small clusters are seen to grow into larger islands in these 5.5-μm low-energy electron microscope images. Atom-high steps separate the alternating light and dark regions; the contrast results from a 90° rotation of the ordered-atom arrangement across the steps. **(a)** Small white elliptical clusters form after 0.1 Si monolayer is adsorbed at room temperature, and the temperature raised for 50 s to 670°C. **(b)** 350 s later, the image shows the effect of "ripening," in which larger islands appear to have swallowed smaller ones. **(c)** A numerical mean-field model, including different chemical potentials in cells around each island, evolved to this configuration, a nearly perfect prediction of the experimental progression. (Adapted from ref. 6.)

quences acquired over the range of temperatures from 640°C to 1210°C.6 He convincingly demonstrated a linear dependence of the inverse amplitude on λ^2 in agreement with the prediction of attachment/detachment limited kinetics. Remarkably, those observations confirmed that the conventional static picture of surfaces is not at all correct. Instead, huge numbers of atoms move back and forth across the surface on a time scale of seconds. It also turns out that two different types of steps can be distinguished on the Si(001) surface. The origin of this difference is the relative orientation between a step and the anisotropic reconstruction; that reconstruction consists of rows of atom pairs that have shifted together to allow overlapping dangling bonds. The two types of steps have different values of step free energy, or "stiffness," leading to different fluctuation amplitudes observable in the LEEM data. Using the measured stiffness of both types of steps as a function of temperature, Bartelt determined precisely the fundamental energies that govern the motion of steps on the surface.

Island hopping

Wolfgang Theis, Bartelt and Tromp⁶ also studied the "ripening" that occurs on Si at sufficiently high temperature as larger islands grow at the expense of smaller islands on the surface. The well-known Gibbs-Thomson effect, in which the chemical potential of an island is proportional to the inverse of its radius of curvature, explains the ripening. Figures 3a and 3b show LEEM snapshots of how a configuration of islands coexisting on the surface has evolved. One might guess that the time dependence of the island sizes could be predicted from a mean-field model, in which a uniform chemical potential describes the sea of atoms diffusing from island to island. As it turned out, that idea was nearly correct: Starting with a refined approximation—allowing the chemical potential in different cells around each island to take on different values, depending on island sizes—the model becomes essentially perfect. Compare the experimental measurement in figure 3b with the results from computations in figure 3c. What's striking is that the model takes kinetic and energy parameters obtained from thermal step fluctuations and successfully predicts the histories of in-

Those observations highlight the importance of the

sea of detached atoms, always present on surfaces at finite temperature. Although this "adatom lattice gas" is too dilute and too mobile to be observed directly, Tromp and Marian Mankos⁶ successfully measured its density. They analyzed the appearance of islands on extremely large step-free regions of a lithographically altered Si(001) surface subsequent to an abrupt drop in temperature. Presumably, those islands were made up of atoms in the adatom lattice gas phase before the temperature was dropped. Measuring the sizes of the islands, the researchers were able to extract the concentration of Si atoms on the surface as a function of temperature. A simple Arrhenius model indicates that the diffusing species on the surface are not isolated atoms at all, but pairs of atoms, or dimers. These same dimers are known from STM images to line up in rows and form the anisotropic reconstruction mentioned above.

Self-assembly

Many of the early experiments—and those showcased in this article so far—concentrated on Si surfaces because of Si's technological importance and the ease with which flat, atomically clean Si surfaces can be prepared. However, a number of groups have investigated the evolution of metal surfaces during deposition, alloying, or relaxation toward equilibrium. A striking example of the rich variety of phenomena that can occur as an alloy system orders comes from recent work by Gary Kellogg's group at Sandia National Laboratories.7 Using LEEM, those researchers observed self-assembly on the nanometer scale during the deposition of lead vapor onto an atomically clean (111) surface of copper at 400°C. Initially, the deposition of lead at that temperature forms a disordered Pb-Cu alloy. Once the alloy covers the surface, additional Pb beads up into compact, nearly circular 70-nm islands. As the coverage increases, the islands begin to order into a hexagonal pattern that Richard Plass describes as a droplet phase (figure 4a). After still more coverage, the islands coalesce into a configuration of stripes (figure 4b) and then into an arrangement of holes in the lead matrix; that arrangement constitutes the so-called negative droplet phase (figure 4c).

The still images, acquired over several minutes, do not convey the richness of the structures' evolution: the nucleation of droplets containing tens of thousands of atoms occurring in a single 30-ms frame. Observation of individual droplets reveals that the islands move within a force field corresponding to dipole—dipole interactions. That motion is consistent with the idea that the interaction forces between islands are mediated by strain fields generated within the substrate. It is remarkable, and perhaps unexpected, that this behavior depends on a high mobility of solid, crystalline islands that contain hundreds of thousands of Pb atoms. The discovery of self-assembly on a mesoscopic-length scale highlights the advantages of LEEM with its unique combination of high data rate and control of the sample environment.

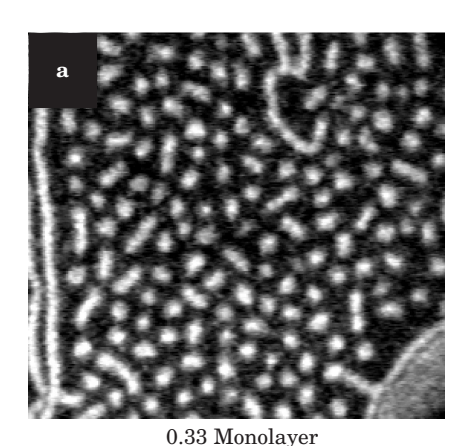
Magnetic phenomena

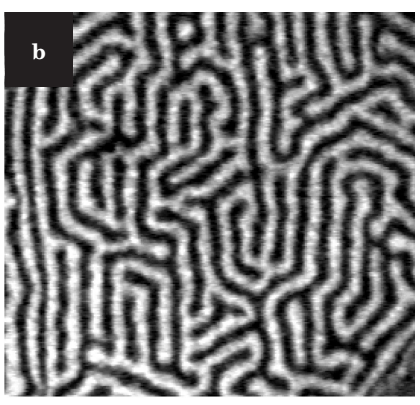
The examples discussed so far illustrate what sort of surface features-atomic steps and domains of different atomic structure, for instance—produce strong contrast using conventional LEEM sources. A spin-polarized electron source extends LEEM's sensitivity to include magnetic phenomena. When a spin-polarized beam of low-energy electrons illuminates a magnetized surface, the reflectivity of that surface can vary dramatically, depending on the relative orientation between the spin of the scattering electrons and the magnetization vector. Bauer's group pioneered the use of this exchange-scattering asymmetry for imaging by developing the first spin-polarized LEEM, or SPLEEM.8 In these microscopes, the spin-polarization orientation of the illuminating electron beam is adjustable. So, comparing a set of images that were recorded using different beam polarizations permits the determination of the local orientation of the magnetization vector in magnetic domains. Usually, one first uses opposite polarization alignments of the illuminating beam to record two LEEM images, and then forms a pixel-by-pixel difference image. This method enhances magnetic contrast, while simultaneously suppressing other LEEM contrast mechanisms. Since the instrument records pairs of images, the SPLEEM technique is marginally slower than conventional LEEM, but shares the advantages of an easily variable sample environment.

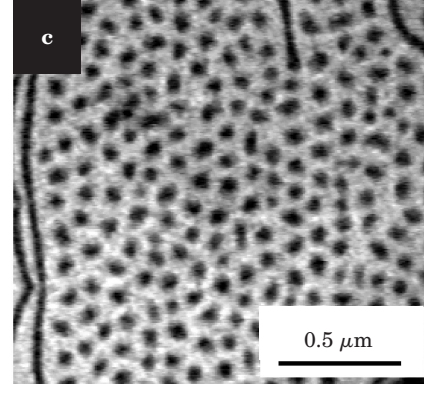
In situ sample processing is particularly interesting for magnetic materials, because magnetic properties depend very sensitively on microstructure. And SPLEEM offers the capability to track the evolution of both structural and magnetic properties simultaneously. For example, Thomas Duden summarized in a recent review⁹ how magnetic thin films and multilayers can be grown in situ while one simultaneously records LEEM images of the sample morphology and SPLEEM images of the exchange-scattering asymmetry.

How magnetic microstructure responds to changing conditions of temperature or externally applied fields is an important question for both applied and basic physics. Using a SPLEEM at Lawrence Berkeley National Laboratory, Helmut Poppa and one of us (Schmid) recently demonstrated the feasibility of operating the instrument while simultaneously applying a controllable magnetic field to the sample. 10 A particularly interesting case of field-dependent magnetic domain patterns occurs in thinfilm samples having a magnetic anisotropy perpendicular to the film. Figure 5a shows a typical SPLEEM image of the zero-field domain structure of a 2.5-monolayer-thick film of iron on Cu(100) at approximately 42°C. Under those conditions, the sample magnetization alternately pointed up and down in a regular pattern of dark and bright stripe domains. When a weak magnetic field was applied perpendicular to the film plane—parallel and antiparallel to magnetizations of the stripes—stripe domains whose magnetization aligned with the applied field simply grew in width at the expense of antialigned stripes. One might imagine that, as a function of increasing field, the aligned stripes would continue growing and eventually form one single large domain. However, that did not happen. In sufficiently large fields, typically at around 1 mT for the temperatures and film thickness in the experiment, the stripe domain patterns became unstable and we found transitions to magnetic droplet and inverse droplet phases.

It is no coincidence that images of the magnetic domain patterns in figure 5 look similar to the compositional domain patterns found in the Pb–Cu surface alloy of figure 4. The compositional and magnetic domain patterns are both stabilized by long-range, dipolar repulsive forces that compete with short-range ordering forces. The distance dependence of magnetic dipolar interactions has the same form as the distance dependence of the strain fields that cause repulsions in the surface alloy phase. In both systems, the competing forces drive the system toward minimum energy configurations consisting of the ordered, equilibrium domain







0.38 Monolayer

0.48 Monolayer

Figure 4. Surface-alloy patterns of lead self-assembling on copper(111). As more lead adsorbs onto the surface, low-energy electron micrographs indicate the formation of **(a)** droplets (at 0.33 monolayer of Pb), **(b)** stripes (0.38 monolayer), and **(c)** inverted-droplets or holes (0.48 monolayer). Images were recorded using 18-eV electrons, with about 400 s separating each picture. The Pb overlayer phase appears bright and the surface alloy phase appears dark. With a full monolayer of lead, the inverted droplets disappear. (Adapted from ref. 7.)

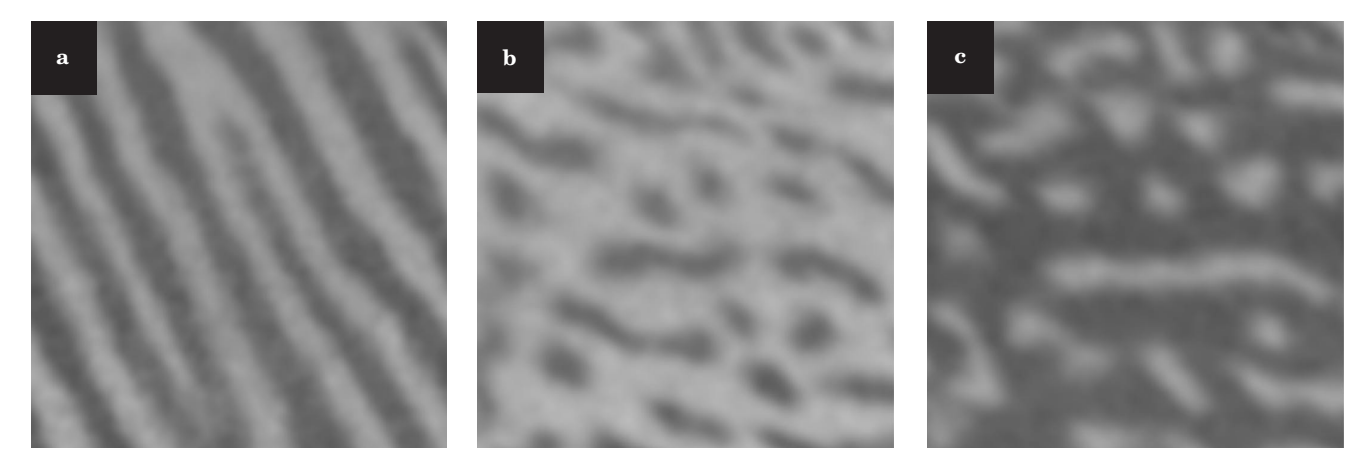


Figure 5. Magnetic domains as seen with spin-polarized, low-energy electron microscopy. Taken from a $4.3 - \mu m \times 4.3 - \mu m$ area of a thin iron film on a copper substrate, these micrographs follow the changes of magnetic domain phases under the influence of a weak magnetic field. (a) A 2.5-monolayer-thick Fe–Cu(100) film at room temperature and zero field shows a magnetic stripe phase. A magnetic field of +1.19 mT in (b) and -1.02 mT in (c) applied to Fe–Cu(100) films produces magnetic droplet and inverse droplet phases, respectively. The evident similarity of transitions between stripe and droplet phases observed in this figure and the alloy compositional domains in figure 4 is explained by the similar form of the force fields governing the two cases.

patterns. In fact, general models for two-phase, two-dimensional systems with dipolar interactions explain exactly the type of pattern formation behavior observed in these two rather different systems.¹¹ Such models predict stable striped domain patterns when the area fraction of the two domain types is near 1/2, while for relative domain area fractions around 1/3 and 2/3, droplet and inverse droplet phases, respectively, should be observed.

Future directions

Remaining challenges in LEEM involve improving the spatial resolution and pushing the time resolution from milliseconds to nanoseconds or better. With spatial resolution presently better than 50 Å, the LEEM built by Tromp at IBM12 approaches the limit imposed by the accelerating field of the objective lens. The SMART project at Bessy II (Berlin Electron Storage Ring Society for Synchrotron Radiation) uses an electron mirror to correct for the aberrations of the objective lens; researchers predict resolution approaching 10 Å or better with such corrections. 13 A second approach, investigated at the University of Mainz in Germany by Gerd Schönhense and his group, aims to achieve a similar result by using carefully tuned time-varying electrostatic fields. 14 Finally, researchers are exploring stroboscopic techniques to track very fast repetitive processes at surfaces. The Mainz group, for instance, is using a pulsed x-ray light source to image the switching of magnetic domains.

In addition to the applications from examples provided in this article, a number of other exciting studies are filling the literature: temperature- or impurity-driven faceting of initially uniform surfaces, structural phase formation and separation during the growth of organic semiconductor thin films, and phase separation during surface chemical reactions, among others. For a more extensive list, interested readers may consult the reviews in references 12 and 15, the Web site at http://www.leemuser.com, and the proceedings of three international workshops held on LEEM and the related technique of photoemission electron microscopy. In PEEM, a UV or soft x-ray light source replaces the incident electron beam, and photoelectrons provide the chemical and surface po-

tential contrast.¹⁷ There are now working microscopes in several laboratories in the US, Europe, Hong Kong, and Japan, and the list of applications continues to grow. With the capability of probing surfaces with high spatial, temporal, spin, and energy resolution, LEEM, SPLEEM, and PEEM each promise to vastly expand our understanding of dynamics at solid surfaces.

It is a pleasure to acknowledge Norm Bartelt for his careful reading and detailed comments on this overview article.

References

- 1. W. Telieps, E. Bauer, Surf. Sci. 162, 163 (1985).
- K. Takayanagi, Y. Tanishiro, S. Takahashi, M. Takahashi, Surf. Sci. 164, 367 (1985).
- R. J. Phaneuf, Y. Hong, S. Horch, P. A. Bennett, Phys. Rev. Lett. 78, 4605 (1997).
- P. A. Bennett, M. Copel, D. Cahill, J. Falta, R. M. Tromp, Phys. Rev. Lett. 69, 1224 (1992).
- J. B. Hannon, F. J. Meyer zu Heringdorf, J. Tersoff, R. M. Tromp, *Phys. Rev. Lett.* 86, 4871 (2001).
- N. C. Bartelt, R. M. Tromp, E. D. Williams, *Phys. Rev. Lett.* 1656 (1994); W. Theis, N. C. Bartelt, R. M. Tromp, *Phys. Rev. Lett.* 3328 (1995); R. M. Tromp, M. Mankos, *Phys. Rev. Lett.* 1050 (1998).
- R. Plass, J. A. Last, N. C. Bartelt, G. L. Kellogg, Nature 412, 875 (2001).
- M. S. Altman, H. Pinkvös, J. Hurst, H. Poppa, G. Marx, E. Bauer, *Mater. Res. Soc. Symp. Proc.* 232, 125 (1991).
- 9. T. Duden, E. Bauer, J. Electron Microsc. 47, 379 (1998).
- H. Poppa, E. D. Tober, A. K. Schmid, J. Appl. Phys. 91, 6932 (2002)
- 11. K.-O. Ng, D. Vanderbilt, Phys. Rev. B 52, 2177 (1995).
- 12. R. M. Tromp, IBM J. Res. Dev. 44, 503 (2000).
- 13. R. Wichtendahl, et al., Surf. Rev. Lett. 5, 1249 (1998).
- 14. G. Schönhense, H. Spiecker, J. Vac. Sci. Technol. B, in press (2002).
- E. Bauer, Rep. Prog. Phys. 57, 895 (1994); Surf. Rev. Lett. 5, 1275 (1998).
- 16. The proceedings of the first three International LEEM/PEEM workshops have been published in *Surf. Rev. Lett.* **5**(6) (1998); *Surface Sci.* **480**(3) (2000); *J. Vac. Sci. Technol. B* **20**(6) (2002).
- 17. S. Günther, B. Kaulich, L. Gregoratti, M. Kiskinova, *Prog. Surf. Sci.* **70**, 187 (2002).

55